General Disclaimer

One or more of the Following Statements may affect this Document

- This document has been reproduced from the best copy furnished by the organizational source. It is being released in the interest of making available as much information as possible.

- This document may contain data, which exceeds the sheet parameters. It was furnished in this condition by the organizational source and is the best copy available.

- This document may contain tone-on-tone or color graphs, charts and/or pictures, which have been reproduced in black and white.

- This document is paginated as submitted by the original source.

- Portions of this document are not fully legible due to the historical nature of some of the material. However, it is the best reproduction available from the original submission.

17

NA-4526

A Facsimile Report

Reproduced by
UNITED STATES
ATOMIC ENERGY COMMISSION
Division of Technical Information
P.O. Box 62 Oak Ridge, Tennessee 37830

Sqt-64760

Distributed: October 1970

LA-4526-MS
SPECIAL DISTRIBUTION

LOS ALAMOS SCIENTIFIC LABORATORY
of the
University of California
LOS ALAMOS • NEW MEXICO

CMF-13 Research on Carbon and Graphite

Report No. 14

Summary of Progress from May 1 to July 31, 1970*

by

Morton C. Smith

*Supported in part by the Office of Advanced Research and Technology of the National Aeronautics and Space Administration.

REPORT NO. 14: SUMMARY OF PROGRESS FROM MAY 1 TO JULY 31, 1970

by

Morton C. Smith

I. INTRODUCTION

This is the fourteenth in a series of progress reports devoted to carbon and graphite research in LASL Group CMF-13, and summarizes work done during the months of May, June, and July, 1970. It should be understood that in such a progress report many of the data are preliminary, incomplete, and subject to correction, and many of the opinions and conclusions are tentative and subject to change. This report is intended only to provide up-to-date background information to those who are interested in the materials and programs described in it, and should not be quoted or used as reference publicly or in print.

Research and development on carbon and graphite were undertaken by CMF-13 primarily to increase understanding of their properties and behavior as engineering materials, to improve the raw materials and processes used in their manufacture, and to learn how to produce them with consistent, predictable, useful combinations of properties. The approach taken is microstructural, based on study and characterization of natural, commercial, and experimental carbons and graphites by such techniques as x-ray diffraction, electron and optical microscopy, and porosimetry. Physical and mechanical properties are measured as functions of formulation, treatment, and environmental variables, and correlations are sought among properties and structures. Raw materials and manufacturing techniques are investigated, improved, and varied systematically in an effort to create specific internal structures believed to be responsible for desirable combinations of properties. Prompt feedback of information among these activities then makes possible progress in all of them toward their common goal of understanding and improving manufactured carbons and graphites.

Since its beginning, this research has been sponsored by the Division of Space Nuclear Systems of the United States Atomic Energy Commission, through the Space Nuclear Propulsion Office. More recently additional general support for it has been provided by the Office of Advanced Research and Technology of the National Aeronautics and Space Administration. Many of its facilities and services have been furnished by the Division of Military Application of AEC. The direct and indirect support and the guidance and encouragement of these agencies of the United States Government are gratefully acknowledged.

II. SANTA MARIA COKE

A. Previous Work

Continuing investigations of Santa Maria coke and of isotropic graphites made from it have been summarized in Reports 9 through 13 in this series.

B. Determination of Calcining Temperatures (R. J. Imprescia, J. A. O'Rourke)

An investigation of the effects of heat-treating temperature on the crystalline parameters of Santa Maria

coke was described in Report No. 11 in this series, and additional data were given in Report No. 12. Fig. 1 is a plot of the effect of calcining temperature up to 1500°C on crystallite thickness, L_c. It is similar to the low-temperature region of Fig. 1 of Report No. 11, but includes data collected since that report was prepared. The furnace atmospheres in which the heat-treating was done are indicated on the figure.

Several outstanding experimental graphites have been made from one particular Santa Maria coke filler, identified as CMF-13 Lot No. CP-8(900)b. This was prepared by vacuum-calcining green Santa Maria at a nominal 900°C and then grinding it in two stages of hammer milling. Because the supply of this filler was small, several attempts were made to reproduce it by grinding Santa Maria LV coke, which had been calcined by its producers at "about 1800°F" (982°C). None of these attempts was successful.

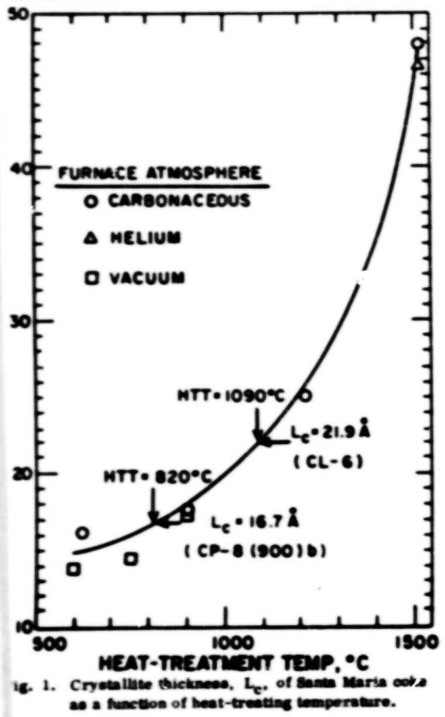

Fig. 1. Crystallite thickness, L_c, of Santa Maria coke as a function of heat-treating temperature.

Recent x-ray measurements on these two cokes have given L_c values of 16.7 Å for Lot CP-8(900)b and of 21.9 Å for the LV coke. As is indicated in Fig. 1, these represent actual heat-treatment temperatures of about 820°C for the coke calcined by CMF-13 and about 1090°C for the LV coke. This difference in calcining temperatures, approximately 270°C, is more than three times as great as that which had been supposed to exist. On the basis of recent studies of the effect of calcining temperature on the grindability of Santa Maria coke, it is clearly sufficient to account for the difference in grinding behavior of these two lots of material and for the inability to reproduce the particle-size distribution of Lot CP-8(900)b by grinding the LV coke.

C. Effects of Calcining Temperature on Properties (R. J. Imprescia)

A series of hot-molded graphites has been made from fillers which were prepared by calcining lump Santa Maria coke at a series of temperatures up to about 2800°C and then grinding them by a standard "S-T-I" schedule--which involved two stages of hammer milling and one of fluid-energy milling. (Details of the preparation of these fillers and their particle-size distributions are given in Report No. 11, pp. 2-6.) The binder used was Barrett grade 30MH coal-tar pitch, the hot-molding cycle was "Program A," and all specimens were graphitized to 2800°C in flowing argon.

To determine binder requirements, preliminary runs were made with selected fillers representing the whole range of heat-treating temperatures. The greatest optimum binder concentration calculated from any of these was about 26 pph. As is discussed in a later section, for maximum packing density at a given molding pressure it is necessary that the binder concentration equal or exceed the calculated optimum. Therefore, binder concentration was held constant at 26 pph for all graphites in this series.

Manufacturing data for these graphites are given in Table I. For specimen 66E-1, made from coke calcined at 620°C, it was impossible to determine accurately the binder optimum, binder residue, and packed filler density because of weight loss from the filler during hot-molding

TABLE I

MANUFACTURING DATA, HOT-MOLDED SANTA MARIA GRAPHITES, SERIES 66 (1)

Specimen No.	Filler Identification	Filler Calcining Temp., °C	Calculated Binder Optimum, pph	Binder Residue (Baked), %	Density, g/cm³ Packed Filler (Baked)	Density, g/cm³ Bulk Baked	Density, g/cm³ Bulk Graph.	Dimensional Change, Baked to Graphitized, % Δℓ	Δd	Δv	Specimen Appearance
66E-1	CL-4	620	---	---	---	1.580	1.853	-7.7	-6.5	-19.3	Circumferential cracks
66F-1	CL-6	1215	26.1	68.6	1.441	1.698	1.788	-5.7	-3.3	-10.0	Good
66G-1	CL-6	1515	28.5	58.9	1.429	1.663	1.718	-2.5	-1.9	-6.0	Radial cracks
66H-1	CL-6	1833	25.7	60.9	1.493	1.748	1.779	-0.7	-0.9	-2.5	Radial cracks
66I-1	CL-6	2147	24.3	59.8	1.[illegible]	1.785	1.799	-0.1	-0.6	-1.3	Good
66J-1	CL-6	2468	23.2	56.1	1.[illegible]63	1.803	1.795	+0.4	-0.2	+0.05	Good
66K-1	CL-6	2808	23.9	64.9	1.556	1.840	1.824	+0.6	-0.1	+0.3	Radial cracks

(1) All fillers were ground by Schedule S-T-I after calcining. Binder in all cases was 26 pph of Barrett 30MH pitch. Molding Program A was used, and graphitization was at 2800°C.

to 900°C. In spite of the indications from preliminary tests, 26 pph of binder was insufficient for coke calcined at 1515°C, and Specimen 66G-1 was deficient in binder. Except for this specimen, the trends of all data in Table I are clear and consistent. Increasing the temperature at which the filler was heat-treated continuously increased both the packed filler density (in the baked condition) and the bulk density in the baked condition. However, since all but one of these fillers had previously been heat-treated to some temperature higher than the baking temperature (900°C), it is apparent that this effect is an indirect one. As was discussed in Report No. 11, the grindability of Santa Maria coke changes with the temperature to which it has been heat-treated, and so does the particle-size distribution of the grinding product. Since these fillers were ground after they were heat-treated, the systematic changes in packed-filler and bulk densities in the baked condition evidently result from systematic differences in size distribution and packing efficiency of the fillers.

Bulk density of the graphitized specimens was high when calcination temperature of the filler was low, diminished to a minimum value as this temperature increased to the region of 1500 to 1800°C, then increased again with still higher heat-treatment temperatures. For low calcination temperatures this behavior is evidently the result of the large shrinkage which accompanies loss of volatile material from incompletely calcined fillers. The volume changes between the baked and graphitized conditions are very large when calcination temperatures are low, resulting in consolidation of the graphite structure. Shrinkage decreases as calcination temperature increases. It is not clear why density increases with heat-treatment temperature of the filler above about 1500 to 1800°C.

Binder residues were generally high, but had no apparent relation to the temperature at which the filler had been heat-treated. Four of the specimens cracked during processing, and this also appeared unrelated to filler treatment or other properties of the graphites.

Samples for physical and mechanical testing are now being machined.

D. Hot-Molded Graphites Made from LV Coke (R. J. Imprescia)

As was described in Report No. 13 in this series, Filler Lot CP-17 was prepared by grinding as-received Santa Maria LV coke (CMF-13 Lot CL-9) in two passes through hammer mills under carefully controlled conditions. Although its particle-size distribution was not

TABLE II

SIEVE ANALYSES OF SANTA MARIA FILLERS, LOTS CP-17 AND CP-17b

Sieve Fraction (U.S. Std. Series)	Weight % in Fraction CP-17	CP-17b
+16	0	0
-16 +25	trace	trace
-25 +45	6.8	6.7
-45 +80	20.0	21.7
-80 +170	31.0	30.0
-170 +325	17.2	17.8
-325	25.0	23.8

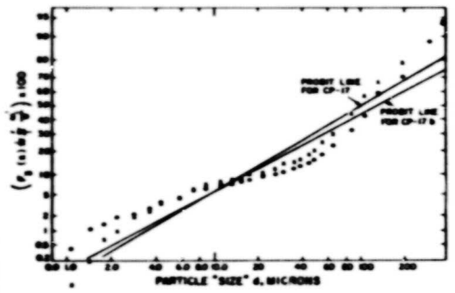

Fig. 2. Log-probability plots of Micromerograph "size" distribution data for filler lots CP-17 and CP-17b.

quite that which was desired, this filler did appear promising for the manufacture of high-quality graphites. Accordingly a second batch of the same lump coke was ground under the same conditions, and the product was identified as Filler Lot CP-17b. Screen analyses of the fillers are given in Table II. As would be expected, they are very similar. The slightly greater proportion of minus 325 mesh fines in Lot CP-17 would not ordinarily be considered significant. The Micromerograph analyses plotted in Fig. 2 indicate that this difference was in particles coarser than about 6 to 8 μ, and that Lot CP-17b actually contained the greater weight fraction of particles finer than 3 to 4 μ.

The curves of Fig. 2 indicate that neither sample is well represented by the lognormal function, so that statistical comparisons should be based on the finite-interval data of Table III rather than the lognormal data. Differences in $\bar{d}_3$, $\bar{d}$, and s_d^2 values between the two grinding products are significant, but the surface-area data of Table IV suggests that the differences are probably unimportant.

Three series of molded graphites have been made from these fillers, to investigate the effects of molding pressure, binder type and concentration, and carbon-black additions. These series are discussed individually in the paragraphs that follow.

Series 65: In this series, hot-molded graphites were made from filler CP-17 using two different binders, three different binder concentrations, and three different molding pressures. The binders were Barrett Grade 23S coal-tar pitch, whose softening point is 54°C, and Barrett Grade 30MH coal-tar pitch, whose softening point is about 110°C. (Other characteristics of these two pitches were compared in Report No. 12 in this series.) Molding temperature was increased at a constant rate of 50°C/hr to 900°C, then held constant at 900°C for 1 hr. All specimens were graphitized at approximately 2800°C in flowing argon. Manufacturing and density data are summarized in Table V.

Only two specimens, 65C-2 and 65A-3, were made using 23S pitch, one with 20 pph and the other with 30 pph of binder. Higher concentrations of binder produced mixes which exploded the dies. Comparison with similar specimens (65D-1 and 65B-1) made using 30MH pitch showed that densities were higher when the higher-viscosity pitch was used. Therefore, all subsequent specimens were made with 30MH pitch.

When the calculated binder optimum for the graphites listed in Table V is plotted against molding pressure, as has been done in Fig. 3, it is clear that when an excess of binder (i.e., 30 pph or 40 pph) is used, packing of filler particles is such that the calculated optimum binder concentration is nearly independent of the binder concentration actually used, and is only weakly dependent on molding pressure. However, when a deficiency of binder

TABLE III

MICROMEROGRAPH SAMPLE STATISTICS FOR FILLER LOTS CP-17 AND CP-17b

LOGNORMAL APPROXIMATION

Sample	$\hat{\mu}_{x3}$	$\hat{\sigma}_x^2$	$\hat{\mu}_x$	$\hat{\mu}_{d_3}$ (micron)	$\hat{\mu}_d$ (micron)	$\hat{\sigma}_d^2$ (micron^2)	S_W (cm^2/g)	CV_d
CP-17b	4.884	2.545	-2.750	471.60	0.228	0.611	862.0	3.43
CP-17	4.574	2.060	-1.607	271.50	0.562	2.161	927.4	2.62

FINITE INTERVAL CALCULATION

Sample	$\bar{x}_3$	s_x^2	$\bar{x}$	$\bar{d}_3$	$\bar{d}$	s_d^2	S_W	CV_d
CP-17b	4.597	0.146	0.169	158.16	1.328	1.432	1103.	0.90
CP-17	4.382	0.261	0.404	134.65	1.787	3.520	1067.	1.05

TABLE IV

SURFACE AREA DATA, FILLER LOTS CP-17 AND CP-17b

Sample	$\bar{S}_W$ (m^2/g)	s_S (1)	d_s (2) (micron)	$\bar{d}$ (Interval Model)	Fuzziness Ratio (3) Lognormal	Interval	ρ (g/cm^3) (He Pycnom)
CP-17b	6.360	0.003	0.502	1.328	73.78	57.66	1.88
CP-17	6.620	0.02	0.512	1.784	67.53	58.67	1.87

(1) Standard Dev. of determinations

(2) $d_s = \frac{6}{\rho S_W}$

(3) Fuzziness Ratio = $\frac{S_W \text{ (BET)}}{S_W \text{ (Calc.)}}$

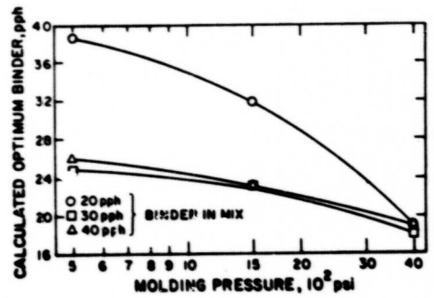

Fig. 3. Calculated optimum concentration of 30MH pitch binder for Series 65 molded graphites.

(i.e., 20 pph) exists, packing of filler particles is less efficient, calculated optima are much higher, and optimum concentration is strongly dependent on molding pressure. This behavior probably results from the lubricating effect of the binder, which, when present in excess, permits filler particles to move past each other in response to the molding pressure, and pack easily to essentially minimum volume. Packed filler density is little affected by binder concentation so long as the binder is present in excess, and the trend of bulk density is similar to that of packed filler density. As would be expected, the greater the excess of binder the lower the carbon residue from it.

TABLE V

MANUFACTURING DATA, HOT-MOLDED SANTA MARIA GRAPHITES, SERIES 65 (1)

Specimen No.	Binder Grade	Binder pph	Molding Pressure, psi	Calculated Binder Optimum, pph	Binder Residue (Baked) %	Density, g/cm³ Packed Filler Baked	Density, g/cm³ Bulk Baked	Density, g/cm³ Bulk Graph.	Dimensional Change, Baked to Graphitized, % Δ ℓ	Δ d	Δ v
65C-2	23S	20	4000	19.3	45.3	1.476	1.610	1.694	-3.8	-3.6	-10.6
65A-3	23S	30	4000	18.8	36.1	1.486	1.646	1.739	-4.2	-3.7	-11.1
65D-1	30MH	20	4000	19.0	55.4	1.488	1.653	1.742	-3.8	-3.6	-10.7
65D-2	30MH	20	1500	31.9	77.1	1.301	1.602	1.699	-4.0	-3.9	-11.4
65D-3	30MH	20	500	38.6	77.3	1.220	1.504	1.592	-4.0	-3.8	-11.2
65B-1	30MH	30	4000	18.1	38.5	1.503	1.677	1.770	-3.8	-3.7	-10.7
65B-2	30MH	30	1500	22.8	45.5	1.427	1.621	1.736	-4.0	-3.8	-11.2
65B-3	30MH	30	500	24.8	52.9	1.398	1.620	1.710	-3.9	-3.7	-10.9
65E-1b	30MH	40	4000	19.3	31.7	1.483	1.671	1.771	-4.1	-3.7	-11.1
65E-2	30MH	40	1500	22.8	37.2	1.427	1.640	1.746	-4.3	-3.9	-11.6
65E-3	30MH	40	500	26.1	41.9	1.379	1.610	1.710	-4.1	-3.9	-11.4

(1) All graphites made from filler CP-17

TABLE VI

MANUFACTURING DATA, HOT-MOLDED SANTA MARIA GRAPHITES CONTAINING THERMAX (1)

Specimen No.	Thermax Addition, pph	Calculated Binder Optimum, pph	Binder Residue (Baked) %	Density, g/cm³ Packed Filler Baked	Density, g/cm³ Bulk Baked	Density, g/cm³ Bulk Graph.	Dimensional Change, Baked to Graphitized, % Δ ℓ	Δ d	Δ v	Specimen Appearance
65B-1	0	18.1	38.5	1.503	1.677	1.770	-3.8	-3.7	-10.7	Good
71C-1	5	14.9	36.2	1.516	1.680	1.790	-4.0	-3.9	-11.4	Good
71A-1	10	17.4	37.1	1.516	1.685	1.797	-4.1	-3.8	-11.2	Radial cracks
71B-1	15	18.1	40.0	1.504	1.685	1.818	-4.4	-4.1	-12.1	Radial cracks

(1) All graphites made from filler CP-17 with 30 pph of Barrett 30MH pitch binder and molding pressure of 4000 psi.

In this series of graphites shrinkage on graphitization was essentially independent of binder type, binder concentration, and molding pressure. This was not true of the molded graphites discussed in Report No. 13, pp. 5-7.

The density data of Table V shows no significant differences between graphites molded at the same pressure with varying proportions of excess binder (although a binder deficiency significantly reduced density). This may not be true of the other properties of these graphites, which are now being investigated.

Series 71: The three specimens of this series were made to investigate the effects of additions of Thermax carbon black to the mix. Like Series 65, these graphites were produced from filler CP-17 and Barrett 30MH pitch binder, molded at 4000 psi with the same temperature program, and graphitized in argon--in this case to 2710°C. Manufacturing and density data are summarized in Table VI,

TABLE VII

MANUFACTURING DATA, HOT-MOLDED RESIN-BONDED SANTA MARIA GRAPHITES, SERIES 68 (1)

Specimen No.	Binder Identification	Binder pph (2)	Molding Pressure, psi	Calculated Binder Optimum, pph	Binder Residue (Baked), %	Density, g/cm³ Packed Filler Baked	Density, g/cm³ Bulk Baked	Density, g/cm³ Bulk Graph.	Dimensional Change, Baked to Graphitized, % Δ ℓ	Δ d	Δ v
68A-1	Varcum 8251	20	4000	20.4	32.0	1.413	1.504	1.615	-4.4	-4.4	-12.7
-2	Varcum 8251	20	1500	23.8	33.6	1.356	1.447	1.567	-4.6	-4.8	-13.8
-3	Varcum 8251	20	500	25.3	35.5	1.331	1.425	1.548	-4.7	-4.7	-13.5
68B-1	EMW 1600	20	4000	16.9	37.0	1.475	1.584	1.699	-4.4	-4.2	-12.3
-2	EMW 1600	20	1500	22.5	36.1	1.377	1.477	1.518	-4.7	-3.8	-13.3
-3	EMW 1600	20	500	24.3	39.9	1.348	1.456	1.591	-5.0	-5.0	-14.3
68C-1	EMW 287	20	4000	20.8	30.5	1.406	1.492	1.603	-4.4	-4.3	-12.5
-2	EMW 287	20	1500	24.1	36.7	1.351	1.450	1.571	-4.6	-4.6	-13.3
-3	EMW 287	20	500	28.9	37.1	1.278	1.373	1.495	-4.7	-4.8	-13.6
68D-1	Varcum 8251	25	4000	27.7	58.0	1.295	1.483	1.599	-4.5	-4.5	-12.9
-2	Varcum 8251	25	1500	31.0	57.4	1.249	1.428	1.522	-4.3	-4.4	-11.8
-3	Varcum 8251	25	500	39.7	58.1	1.165	1.335	1.446	-4.8	-4.7	-13.5
68E-1	EMW 1400	25	4000	16.2	22.2	1.490	1.573	1.683	-4.3	-4.1	-11.9
-2	EMW 1400	25	1500	17.7	29.0	1.462	1.568	1.703	-4.9	-4.6	-13.4
-3	EMW 1400	25	500	19.1	32.3	1.436	1.552	1.702	-5.0	-4.9	-14.1
68F-1 (3)	EMW 287	25	4000	15.4	30.3	1.505	1.619	---	---	-4.5	---
-2	EMW 287	25	1500	18.0	33.8	1.455	1.578	1.713	-4.9	-4.5	-13.3
-3 (4)	EMW 287	25	500	18.7	40.7	1.442	1.588	1.741	-5.0	-4.9	-13.5

(1) All graphites made from filler CP-17b

(2) Including 1% maleic anhydride curing catalyst

(3) Specimen cracked through the center of its length during graphitizing and some fragments were lost

(4) Specimen cracked into 3 pie-shaped pieces during graphitizing

in which data for specimen 65B-1, containing no carbon black, are repeated for comparison.

From Table VI it appears that additions of 5, 10, or 15% Thermax had little effect on packed-filler and bulk densities in the baked condition. Bulk density after graphitizing increased with increasing Thermax content. Shrinkage during graphitization was increased by the presence of the Thermax, which is probably related to the fact that the specimens containing 10 and 15% Thermax cracked during hot-molding.

Specimens for physical and mechanical properties measurements are now being machined from these graphites.

Series 68: The graphites of Series 68 differed from those of Series 65 primarily in the binders used, which were furfuryl alcohol resins instead of coal-tar pitches. Filler CP-17b was also substituted for CP-17 but, as is discussed above, these two fillers are very much alike and this is not considered a significant change. Molding and graphitizing procedures were the same as for Series 65.

The four binders used to make the Series 68 graphites were commercial furfuryl alcohol resin, Varcum 8251, with viscosity of 250 cp, and three experimental resins

synthesized in CMF-13: EMW 1400, viscosity 1400 cp; EMW 1600, viscosity 1600 cp; and EMW 287, viscosity 9200 cp. In all cases 1% maleic anhydride was included in the binder as a curing catalyst. Manufacturing and density data are summarized in Table VII.

Comparing these data with those of Table V for pitch-bonded graphites, it is seen that the resin-bonded graphites have lower packed-filler densities than do the corresponding pitch-bonded ones. Apparently the lubricating properties of the furfuryl alcohol resins are not as good as those of the coal-tar pitches so that, at the same molding pressure, less efficient filler-particle packing is achieved. Packing density of the resin-bonded materials did, however, increase as molding pressure was increased, and bulk density in the baked condition followed a similar trend.

The resin-bonded graphites also tended to shrink more during graphitization than did the corresponding pitch-bonded ones. Unlike the pitch-bonded specimens, the resin-bonded graphites showed increasing shrinkage with decreasing molding pressure. This is probably related to lower packing densities in the resin-bonded materials, and their consequent ability to accomodate more shrinkage of the binder residue.

For the graphitized condition, density varied not only with molding pressure but also with resin viscosity and concentration, indicating an interaction between packing of filler particles and shrinkage of binder residues. For the 68A, 68B, and 68C graphites, which contained 20 pph of binder and in general were binder-deficient, graphitized density decreased with decreasing molding pressure, decreasing packed-filler density, and increasing binder deficiency. For specimens containing 25 pph of binder (68D, 68E, 68F), the trend of graphitized density varied with the viscosity of the binder. When Varcum 8251 (250 cp) was used, packed-filler densities were very low, and graphitized densities decreased with molding pressure. With EMW 1400 (1400 cp) packed-filler densities were higher and bulk density after graphitization was nearly independent of molding pressure. With EMW 287 (9200 cp) graphitized density increased as molding pressure was reduced.

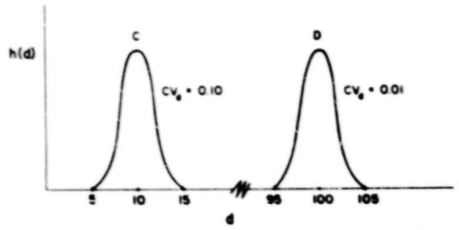

Fig. 4. Representation of two normal distributions having different means and equal variances.

Graphitized densities of the resin-bonded specimens were generally low compared with those of the pitch-bonded specimens of Series 65. The highest final density of any of these resin-bonded graphites was 1.741 g/cm^3 for specimen 68F-3, which was bonded with 25 pph of the highest-viscosity resin and molded at only 500 psi. The corresponding specimen containing only 20 pph of the same resin (specimen 68C-3) had graphitized density of only 1.495 g/cm^3. Volume shrinkages of the two specimens were nearly the same, about 12.5%. The difference was principally in packed-filler densities, which were 1.442 g/cm^3 when 25 pph of binder were used and only 1.278 g/cm^3 when binder concentration was 20 pph. It is evident that the lubricating property of the binder is extremely important with regard to compaction behavior of the filler and density of the finished graphite, and that, especially when the binder has low lubricity, a deficiency of binder has very serious effects on compaction and density.

Specimens are now being machined to determine the effects of these variables on properties other than density.

E. Extruded Santa Maria Graphites

Extruded graphites made with Santa Maria fillers are discussed below in connection with research on binders.

II. PARTICLE PACKING

A. Theory (H. D. Lewis)

One of the major parameters that controls the fabrication behavior and properties of any initially particulate system, including most ceramic and powder-metallurgy products as well as carbons and graphites, is the packing behavior of the solid particles of which it is principally composed. A few generalizations can be made concerning particle packing, simply on the basis of experience and empirical observations. So far, however, there is no rational method for even a semiquantitative prediction of the packing behavior of a given powder based on the measurable properties of its particles.

In an attempt to improve this situation, Lewis and Goldman (J. Amer. Cer. Soc. 49, 323, 1966, and LASL Report LA3656, 1967) have proposed a "maximum variance, coefficient of variation" model of the packing of particulate solids. The development of the model was intuitive, and was based on the concept that a broader distribution of particle sizes--represented by a larger value of s_d, the variance of the distribution--would improve the probability that small particles would fill the voids between larger ones, and would therefore increase packing density. However, as is illustrated by Fig. 4, two powders having normal particle-size distributions may have the same variance and still differ widely in their degree of "monosizedness". Thus, most of the particles in the distribution having a mean particle diameter ($\bar{d}$) of 100 μ have diameters within ±5% of the mean, while in the distribution whose $\bar{d}$ is only 10 μ the corresponding range is ±50% of the mean. The latter distribution would be expected to pack to higher density. Because of this, Lewis and Goldman used the coefficient of variation of the particle-size distribution, $CV_d = s_d/\bar{d}$, to predict packing behavior rather than using the variance alone.

The Lewis-Goldman model simply predicts that particulate systems having larger values of CV_d will pack to higher bulk densities. It assumes that the particles do not deform appreciably during compaction, and the statistical treatment assumes lognormal particle-size distributions, implying positive skewness in the distribution of particle sizes. It does not provide a method for computing the bulk density of a compact made from a given powder. However it does provide a statistical procedure for ranking individual powders or mixtures of powders according to their coefficients of variation and so, presumably, in the order of the packed density that they will attain under a given set of compaction conditions. Thus it provides a criterion for selecting among different powders or selecting a weight ratio in which two powders should be combined in order to produce maximum packing density.

During the past two years experimental evidence has been gathered which indicates quite convincingly that CV_d is a reliable measure of the relative packing densities to be expected of particulate systems. (Some of the evidence is discussed in the next section of this report.) However, no mathematical verification of the validity of the "maximum variance, coefficient of variation" model has existed. Therefore an attempt has recently been made to produce an analytical demonstration that it was correct.

During the past ten years, several prominent statisticians have published articles on random space-filling. In most cases the problem considered has been that of determining the average number of line segments of length d which could be placed at random, without overlap, on a line segment of length x, where x is much greater than d. The simplest situation is that in which length d of the line segments is constant. Analytical solutions to this problem have been derived by P. E. Ney (Ann. of Math. Stat., 33, 702, 1962) and by A. Renyi (Publ. Math. Inst. Hung. Acad. Sci., 3, 109, 1959). Attempts to extend it to two dimensions have been made by I. Palasti (Publ. Math. Inst. Hung. Acad. Sci., 5, 1960) and by H. Solomon (Dept. Stat., Stanford Univ., Tech. Report No. 148, 1969). These authors were concerned with estimating the average number and variability of the number of segments of constant length that could be randomly placed on the line. None of them appear to have considered the case of a distribution of line-segment lengths, or the problem of determining a distributional parameter which is related to packing density on the line.

Although it is obvious that a one-dimensional model is a great oversimplification of the three-dimensional particle-packing problem, it was decided to use this model in an attempt to test the relation between CV_d and packing density. W. M. Visscher, LASL Group T-9,

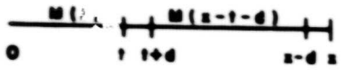

Fig. 5. The one-dimensional packing problem.

after discussion with A. Goldman, derived an analytical solution to the one-dimensional problem for the cases of both monosized and heterogeneously sized particles. The integral equations derived by Visscher are of the same form as those derived by Nye and by Renyi. The sketch of Fig. 5 illustrates the problem considered. A particle of length d is placed at random on the line (one-dimensional container) of length x and occupies the segment (t, t+d). Additional particles are added until no more can be placed on the line without intersection. The solution to the problem is the integral equation

$$M(x) = \int_0^x g(d) \left[\frac{2}{x-d} \int_0^{x-d} M(t)\, dt + 1 \right] dd$$

where: M (x) = mean number of particles on the line
M (t) = mean number of particles on the segment (0, t)
g (d) = probability density function representing the particle-size distribution.

This integral equation is solved by an iterative numerical method, using the facts (proven by Nye, Renyi, and Visscher) that:

$$\lim_{x \to \infty} \frac{M(x)}{x} = C, \text{ and}$$

$$M(x) = Cx - (1 - C) + O\left[\frac{1}{x^n}\right]$$

where $O[1/x^n]$ indicates terms of $1/x^n$ for n very large.

For the case of monosized particles, the packing density calculated in this way is 0.748--that is, 74.8% of the length of the line is finally occupied by short line segments of constant length d. This is surprisingly close to the three-dimensional, close-packed, packing fraction of 0.741 for monosized spheres.

The effect of variations in CV_d was tested for the simple case of the uniform ("rectangular") distribution, in which g(d) = 1/(b - a), where b and a are, respectively, the upper and lower particle-size limits. For this distribution the mean particle size is (b + a)/2 and the variance is $(b-a)^2/12$, so that the maximum value of CV_d is 0.577. Packing density on the line was calculated for several values of a and b, with the results shown in Fig. 6. It was and that as the lower particle-size limit, a, approached zero, packing density increased, as indicated by the several values plotted at CV_d = 0.525. (The two values well above the average curve are probably unrealistic, since they represent cases in which a was extremely small so that many particles could be packed into essentially zero length. The two low values represent cases in which b was large relative to the line length, and so are also probably not representative. However, the average of these extreme cases--represented by the dotted circle--is near the general curve.) For similar mean particle sizes packing density increased continuously with increasing CV_d and, on the average, reached a maximum value near 0.83 when CV_d was a maximum. As CV_d was reduced toward zero, packing density approached the value for the monosized case.

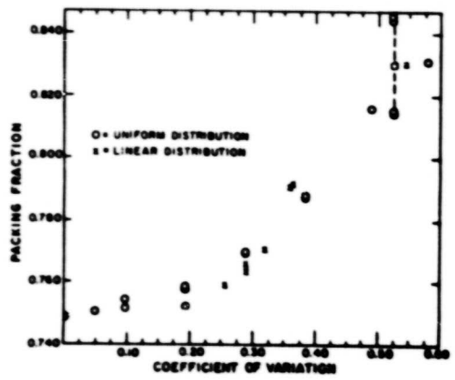

Fig. 6. Packing density on the line related to coefficient of variation for uniform and linear distributions.

Packing densities were also estimated for the linear distribution, g (d) = p + kd, where p and k are constants. These results are also plotted in Fig. 6, and are very similar to those for the uniform distribution. This is not surprising when it is noted that the linear distribution becomes the monosized case when the variance is zero, and when the variance becomes large the linear distribution approaches the uniform distribution with CV_d approaching 0.577.

A few calculations have been made for distributions such that g (d) is defined by lognormal functions. These again showed that packing density increases with CV_d. They also indicated that, as CV_d increases, the packing density approached by lognormal distributions is much higher than those approached by uniform or linear distributions. Evidently the nature of the particle-size distribution must be considered in attempts to find a quantitative relation between packing density and CV_d.

B. Experimental (R. J. Imprescia)

Experimental evaluation of the relation between CV_d and packing density is difficult in the case of graphites for several reasons, related both to the characteristics of the particles and to the changes that occur during manufacturing processes. The filler material usually has a very broad range of particle sizes, in a distribution which is poorly approximated by the lognormal function, and the particles usually exhibit a broad spectrum of shapes. Compaction experiments are affected by springback of the filler, which may be large if the particles are not held firmly in place by the binder. The binder may react with volatile matter in the filler, causing a change in packing characteristics. As has been discussed above, the lubricating action of the binder is important in permitting filler particles to move past each other during compaction, and its effectiveness in doing so varies with both the nature and the concentration of the binder. In hot-molding, if the filler is a coke which has not previously been calcined to above the molding temperature, it may undergo weight loss and shrinkage during molding, which changes its compaction behavior.

In spite of these difficulties, reasonably good packing densities can be determined for carbon fillers by hot-molding experiments, provided that the fillers have been heat-treated to temperatures at least as high as the maximum molding temperature and that at least a sufficiency of binder is present.

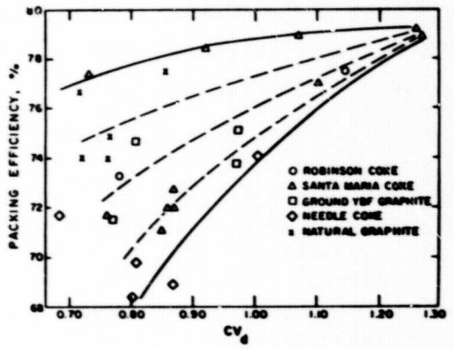

Fig. 7. Packing efficiency as a function of coefficient of variation for five different filler materials.

Packing-density data have been collected from hot-molding experiments on pitch-bonded fillers of five different types. These included: two isotropic fillers--Robinson coke, and a group of Santa Maria cokes; a commercial needle coke; a graphite flour produced by grinding commercial YBF graphite, which is supposedly made from a needle coke; and a ground Ceylon natural graphite. All but one of these fillers had previously been heat-treated to at least 900°C. The exception was filler No. CP-8(900)b, used to make specimen No. 63J-2; however, previous experience with this filler had indicated that very little weight loss occurred when it was hot-molded. All fillers were mixed with a slight excess of Barrett 30MH coal-tar pitch, and molded at 4000 psi in graphite dies to a temperature of 900°C. Density data for the molded specimens in the baked (i.e., hot-molded) condition are summarized in Table VIII and Fig. 7.

Because the densities of filler particles vary both with their internal structures and with the temperatures to which they have been heat-treated, the maximum bulk densities to which various fillers can theoretically be

TABLE VIII

RELATIVE PACKING DENSITY AS A FUNCTION OF COEFFICIENT OF VARIATION FOR HOT-MOLDED, PITCH-BONDED FILLERS

Specimen No.	Filler		Density, g/cm^3		Packing Efficiency, %[a]	CV_d[b]
	Lot No.	Type	Packed Filler	Helium		
35B	T(HCTE)-1	Robinson	1.45	1.87	77.5	1.142
35F	T(HCTE)-17	Robinson	1.37	1.87	73.3	0.780
63J-2	CP-8(569)b	Santa Maria	1.450	1.883	77.0	1.101
63H Series	G-26	Santa Maria	1.612	2.084	77.4	0.729
64G-1	CL-9(W-1)	Santa Maria	1.476	1.870	78.9	1.27
64H-1	CL-9(W-2)	Santa Maria	1.489	1.879	79.2	1.26
64I-1	CL-9(W-3)	Santa Maria	1.487	1.884	78.9	1.07
64J-1	CL-9(W-4)	Santa Maria	1.491	1.889	78.4	0.92
66F-1	CL-6 (1215)	Santa Maria	1.441	2.01	71.7	0.78
66H-1	CL-6 (1833)	Santa Maria	1.493	2.10	71.1	0.85
66I-1	CL-6 (2147)	Santa Maria	1.534	2.13	72.0	0.87
66J-1	CL-6 (2468)	Santa Maria	1.563	2.15	72.7	0.87
66K-1	CL-6 (2808)	Santa Maria	1.556	2.16	72.0	0.86
S-5	T(YBF)-1	YBF Graphite	1.66	2.21	75.1	0.973
S-4	T(YBF)-2	YBF Graphite	1.63	2.21	73.8	0.969
S-3	T(YBF)-4	YBF Graphite	1.65	2.21	74.7	0.807
S-2	T(YBF)-12	YBF Graphite	1.58	2.21	71.5	0.772
36B	T(CN)-1	Needle Coke	1.57	2.12	74.1	1.006
36C	T(CN)-2	Needle Coke	1.52	2.12	71.7	0.684
36D	T(CN)-3	Needle Coke	1.48	2.12	69.8	0.810
36F	T(CN)-5	Needle Coke	1.46	2.12	68.9	0.869
36I	T(CN)-8	Needle Coke	1.45	2.12	68.4	0.803
37B	T(Na)-1	Nat. Graphite	1.76	2.27	77.5	0.856
37C	T(Na)-2	Nat. Graphite	1.74	2.27	76.7	0.716
37D	T(Na)-3	Nat. Graphite	1.70	2.27	74.9	0.766
37E	T(Na)-4	Nat. Graphite	1.68	2.27	74.0	0.721
37F	T(Na)-5	Nat. Graphite	1.68	2.27	74.0	0.762

(a) Packing efficiency = (Packed filler density) ÷ (Helium density)

(b) Determined using the FIMINT Program.

packed are not the same. To compare packing efficiences of different fillers it is therefore necessary to normalize the experimentally determined packed filler densities by means of a parameter which accounts for the bulk densities of individual particles. The normalizing factor used here is "helium density"--i.e., the density of the uncompacted filler particles as determined by helium pycnometry--which is assumed to represent the bulk density that would be attained if the particles were packed to fill space completely. Actually, since helium can enter surface-connected voids too small to be entered by other particles, this is an overestimate of the bulk density that could be attained with perfect packing.) The index of packing efficiency is taken to be the packed filler density of the baked sample divided by the helium density of the filler.

From Fig. 7, it is evident that there is a great deal of scatter in data relating packing efficiency to CV_d, and that the scatter is worse for lower values of CV_d. The trend, however, is clearly that packing efficiency increases with CV_d. It is believed that the scatter results largely from variations in particle shape and in the degree to which voids within the filler particles are connected to particle surfaces. Thus, well-oriented, platelike particles would pack to higher densities than would rounded equiaxed particles, and equiaxed particles to higher densities than less-regular shapes. This might be represented by the "shape-factor bands" suggested by the dashed curves in Fig. 7. Much of the rest of the data scatter can probably be explained on the basis that particles whose internal porosity is largely surface-connected have high helium densities but, if their pore volumes are large, they cannot be packed to produce high bulk density. With such a filler the calculated packing efficiency is misleadingly low.

IV. BINDER CHEMISTRY

A. Polyphenylene Binders (E. M. Wewerka)

Most of the polyphenylenes which have been reported in the literature have been made from benzene or were copolymers of benzene. In general they have been insoluble and infusible. Recently Bilow and his coworkers have reported the copolymerization of biphenyl and m-terphenyl to give a polymer that is less crystalline than those usually obtained from the polymerization of benzene. As expected, the lower degree of intramolecular bonding in this material caused it to have a true melting range and a reasonable degree of solubility. Bilow's work indicated that additional reductions in melting temperature and greater solubility could be obtained by further increasing the degree of molecular disorder in the polymer. To polymerize such irregularities into the polyphenylene system has indeed been the main objective of the CMF-13 work on these materials.

An effort to repeat some of Bilow's work has given unsatisfactory results. Biphenyl and m-terphenyl were copolymerized by Bilow's group from the melt--i.e., the comonomers were melted and polymerized as such, after the addition of a catalyst. Here it has been found that when this procedure was used the reactants soon became too viscous to stir, after which most of the polymerization took place in an uncontrolled, heterogeneous manner.

To alleviate this problem, an attempt is now being made to arrive at polyphenylenes by solvent polymerization of aromatic materials, including benzene, biphenyl, and a mixture of biphenyl and m-terphenyl. It is anticipated that presence of the solvent will result in uniform dispersion of the reactants, catalyst, and product during polymerization. For this purpose the solvent must be either non-aromatic or a nonreactive aromatic, so that it does not itself enter into the polymerization. However, it must be able to dissolve a wide range of aromatic materials.

The initial solvent choice for this purpose was decahydronapthalene. However, even benzene could not be polymerized in this solvent, due apparently to some factor such as a solvent-monomer or solvent-catalyst interaction, a solvent-dipole mismatch, or solvent impurities. An attempt has therefore been made to use nitrobenzene as the solvent for polymerization of benzene. This too has so far been unsuccessful. However, a number of experimental variables remain to be investigated.

B. Synthesis of the Lactone Component (E. M. Wewerka, R. J. Barreras)

One of the byproducts of polymerization of furfuryl alcohol with γ-alumina is thought to be 4-methyl, 4-furfuryl, 2-en, γ-butyrolactone ("γ-BL"). To assure that this identification is correct, an attempt is being made to carry out the independent synthesis of γ-BL, so that the product can be compared with material isolated from the alumina-polymerized furfuryl alcohol resin. At this point two alternative methods are being in-

Fig. 8. Alternative synthetic routes to 4-methyl, 4-furfuryl, 2-en, γ-butyrolactone ("γ-BL").

vestigated, which are illustrated in Fig. 8. The first two steps, which are common to both synthetic schemes, have been completed, and work is progressing on subsequent steps.

A study to determine the manner in which γ-BL is formed during the polymerization of furfuryl alcohol has also been undertaken. A possible intermediate in its formation is α-angelica lactone, and the conditions under which this lactone is produced from levulinic acid are therefore being examined. Various conditions have been tried to effect this transformation in a facile manner, including: use of dehydrating agents (H_3PO_4, γ-Al_2O_3, and $MgSO_4$); altering reaction time (up to 4 hours); and adjusting pressure (atmospheric to 300 torr). None of these has been entirely successful, and the best conditions so far found for the reaction are slow distillation of levulinic acid at atmospheric pressure. Even under these conditions, a considerable amount of resinified material was found in the distilling flask. It is not certain whether this residue was a polylevulinic acid or a polymer of angelica lactone formed through its double bond after initial dehydration.

C. Infrared Investigations of Polymer Components (E. M. Wewerka)

Throughout the investigation of the low-molecular-weight components of furfuryl alcohol resins, infrared spectroscopy has been used as a qualitative tool to aid in the identification of constituents isolated by gas chromatography. Infrared data were available for most of the species expected to appear in these resins, so that direct comparisons of these with the spectra of components isolated here has provided a quick method of component identification. However, no spectral data had previously been compiled for two of the components: 2,5-difurfuryl furan, and 4-methyl, 4-furfuryl, 2-en, γ-butyrolactone (γ-BL). A qualitative correlation has therefore been made of the IR band positions with the structures assigned to these two materials.

It was expected that 2,5-difurfuryl furan would have an IR spectrum similar to that of its lower homolog, difurylmethane. This was the case except for three new

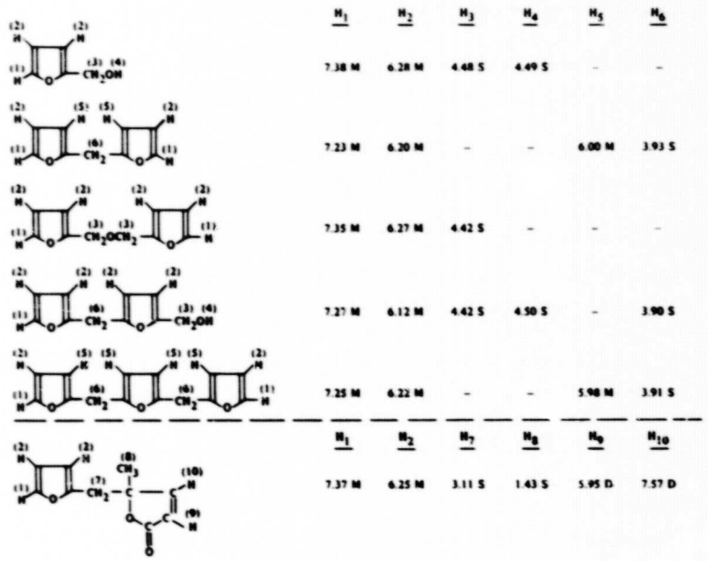

Fig. 9. Assigned nuclear magnetic resonance chemical shifts and multiplicities of the low-molecular-weight constituents of furfuryl alcohol polymers.

bands found at about 1562, 976, and 792 cm^{-1}. Considering the structures of 2,5-difurfuryl furan and difurylmethane, it appears that the 1562 cm^{-1} band is a ring-stretching frequency of the center furan ring. The other two bands are probably due to carbon-hydrogen out-of-plane deformations of the center furan ring, since they appear in a region in which such excitations are usually observed.

The situation for γ-BL is more complicated. In addition to bands expected for the furan system, many others appear in the spectrum of γ-BL, and assignment of an excitation mode to each of them is difficult. However, corroborative evidence for the α, β-unsaturated, γ-lactone structure can be obtained by examining the 1600 to 1800 cm^{-1} region of the spectrum.

A strong carbonyl stretching band peaking at 1755 cm^{-1} is found in the IR spectrum of γ-BL. Its relatively high frequency seems to be characteristic of lactone- or ester-carbonyl groups. More substantial evidence in this respect is the fact that the carbonyl band of γ-BL is nearly identical in both peak shape and position to that of the similar molecule 4,4-dimethyl, 2-en, γ-butyrolactone. Further, the carbonyl band of γ-BL appears similar to those of several other α,β-unsaturated, γ-lactones described in the literature.

Also of interest is a weak band in the γ-BL spectrum at 1603 cm^{-1}, which can be attributed to the conjugated double bond in the lactone ring. Again the spectra of substituted α, β-unsaturated, γ-lactones described in the literature are useful for comparisons. In nearly all instances a band near 1600 cm^{-1} is observed in the spectra of these lactones, providing further information regarding the position of the double bond in the lactone ring of γ-BL.

D. NMR Investigations of Polymer Components (E. M. Wewerka)

Nuclear magnetic resonance (NMR) has been a most

TABLE IX

EFFECTS OF BATCH SIZE ON THE PROPERTIES OF EXTRUDED GRAPHITES

Mix Components		Batch	Bulk Density,	Binder Carbon Residue,	Young's Modulus,	Electrical Resistivity,		Thermal Conductivity,		Coefficient of Thermal Expansion,	
Flour	Binder	Size	g/cm³	%	10^6 psi	μΩ cm		W/cm-°C		in/in/°C (a)	
						WG	AG	WG	AG	WG	AG
G-18	Varc 8251	Small	1.876	46.6	2.52	1170	1897	1.22	0.66	2.69	4.60
G-18	EMW 1600	Small	1.908	49.5	2.57	1105	2059	1.40	0.70	2.50	5.21
Changes			+0.032	+2.9	+0.05	- 65	+162	+0.18	+0.04	-0.19	+0.61
G-18	Varc 8251	Large	1.873	47.3	2.48	1154	2173	1.21	0.64	2.40	4.90
G-18	EMW 1600	Large	1.921	50.6	2.74	1048	2096	1.25	0.72	2.46	5.02
Changes			+0.047	+3.3	+0.26	-106	-123	+0.04	+0.08	+0.06	+0.12
G-29	Varc 8251	Small	1.881	48.6	2.23	1150	1860	1.17	0.71	2.37	4.87
G-29	EMW 1600	Small	1.920	51.0	2.30	1145	1903	1.29	0.72	2.81	4.87
Changes			+0.039	+2.4	+0.07	-5	+43	+0.12	+0.01	+0.44	0.00
G-29	Varc 8251	Large	1.893	47.8	2.34	1145	1943	1.30	0.76	2.84	4.89
G-29	EMW 1600	Large	1.920	51.4	2.40	1145	1914	1.25	0.72	2.43	4.29
Changes			+0.027	+3.6	+0.06	0	-29	-0.05	-0.04	-0.41	-0.60
G-13	Varc 8251	Small	1.880	46.8	2.16	1280	1921	---	---	2.61	4.64
G-13	Varc 8251	Large	1.901	---	2.31	1133	1901	1.26	0.75	2.63	4.24
Changes			+0.021	---	+0.15	-147	-20	---	---	+0.02	-0.40
G-26	Varc 8251	Small	1.863	47.6	1.75	1626	1874	0.81	0.70	5.19	5.48
G-26	EMW 1600	Small	1.906	50.2	1.79	1368	1884	0.91	0.62	4.93	6.04
Changes			+0.043	+2.6	+0.04	-258	+10	+0.10	-0.08	-0.26	+0.56
G-2[illegible]	Varc 8251	Large	1.881	48.1	1.72	1608	---	---	---	---	---
G-2618	EMW 1600	Large	1.902	51.3	1.73	1590	---	---	---	---	---
Changes			+0.021	+3.2	+0.03	-18	---	---	---	---	---

(a) Average, 25-645°C

valuable analytical technique for identifying the components of furfuryl alcohol resins. In Fig. 9 the NMR frequencies assigned to the component molecules are listed. The band positions relative to tetramethyl silane (TMS), called "chemical shifts", are given in parts per million downfield from TMS, with an indication of whether the particular band is a singlet (S), a doublet (D), or a multiplet (M).

V. EXTRUDED GRAPHITES

A. Effects of Batch Size and Binder Type (J. J. Dickinson)

Several relatively large batches of extruded graphite have been made using four different graphite flours and two different furfuryl alcohol resin binders. The effects of batch size and binder type on the properties of graphites made from the various fillers have been evaluated.

TABLE X

ANISOTROPY RATIOS OF EXTRUDED GRAPHITES

Mix Components		Batch	Anisotropy Ratios			Preferred Orientation		Crystalline Parameters	
Flour	Binder	Size	Electrical Resistivity	Thermal Conductivity	Coefficient of Thermal Expansion	M Value	Bacon Index	L_c	d_{002}
G-18	Varc 8251	Small	1.62	1.85	1.71	1.77	1.454	---	---
G-18	EMW 1600	Small	1.86	2.00	2.08	1.81	1.473	---	---
Changes		Small	+0.24	+0.15	+0.37	+0.16	+0.019	---	---
G-18	Varc 8251	Large	1.88	1.89	2.04	1.95	1.471	---	---
G-18	EMW 1600	Large	2.00	1.74	2.04	2.15	1.542	---	---
Changes		Large	+0.12	-0.15	0.0	+0.20	+0.071		
G-29	Varc 8251	Small	1.62	1.65	2.05	1.75	1.435	---	---
G-29	EMW 1600	Small	1.66	1.79	1.73	1.39	1.360	---	---
Changes		Small	+0.04	+0.14	-0.32	-0.36	-0.075		
G-29	Varc 8251	Large	1.70	1.71	1.72	1.48	1.382	480	3.360
G-29	EMW 1600	Large	1.67	1.74	1.77	---	---	---	---
Changes		Large	-0.03	+0.03	+0.05	---	---	---	---
G-26	Varc 8251	Small	1.15	1.16	1.06	0.35	1.090	---	---
G-26	EMW 1600	Small	1.38	1.47	1.23	0.48	1.382	480	3.360
Changes		Small	+0.23	+0.31	+0.17	+0.13	+0.208	---	---

The size of a normal extrusion batch is controlled by the capacity of the mix chamber of the CMF-13 extrusion press, which will hold approximately 900 grams of most graphite mixes. Larger batches are made by blending and chopping the required amount of mix and extruding it in a series of lots of about 900 grams each (as has been described in LASL Report No. LA-3981, and in previous reports in this series). Some variations in properties with batch size have been noted.

The four fillers used in this experiment were: Great Lakes Grade 1008-S graphite flour, CMF-13 Lot No. G-13 (CMB-6 Lot No. M2); Great Lakes Grade 1008-S graphite flour, CMF-13 Lot No. G-18 (CMB-6 Lot No. M3); Great Lakes Grade 1008-S graphite flour, CMF-13 Lot No. G-29 (CMB-6 Lot No. M1), premixed with 15% of Thermax carbon black; and Santa Maria graphite flour, CMF-13 Lot No. G-26 (Y-12 SM1V Blend 1). The two binders were: Varcum 8251, a commercial furfuryl alcohol resin made by diluting a high-viscosity resin with monomer to a final viscosity of about 250 cp; and EMW 1600, a CMF-13 furfuryl alcohol resin made by polymerizing directly to a viscosity of 1600 cp. In all cases the binder contained 4% maleic anhydride as a curing catalyst, and the dry mix composition was 85 parts graphite flour and 15 parts Thermax carbon black.

Properties of the graphites produced are listed in Tables IX and X. The values given are averages representing a number of rods from each batch, and in most cases several measurements on each rod.

With all four of the fillers, substitution of EMW 1600 for Varcum 8251 significantly increased bulk density, binder carbon residue, and Young's modulus. The effect of this change in binder on other properties and on the anisotropy ratios was less consistent. In most cases, however, the use of the more viscous binder increased

TABLE XI

BULK DENSITIES OF SOME ACE4 EXTRUSIONS

Specimen Number	Bulk Density, g/cm^3			
	Full-Length Rod, ≈ 0.475 in. dia	1/3-Length Rod, ≈ 0.475 in. dia	1/2 Length Rod, 0.453 in. dia	1/3-Length Rod 0.250 in. dia
ACE4-26	1.919	1.917	1.919	1.924
ACE4-19	1.918	1.913	1.919	1.920
ACE4-18	1.915	1.913	1.917	1.916
ACE4-12	1.918	1.915	1.920	1.924
ACE4-5	1.914	1.911	1.918	1.920
AC4-21	1.920	1.919	1.920	1.922
ACE4-Avg.	1.917 ± 0.002	1.915 ± 0.003	1.919 ± 0.001	1.921 ± 0.003

the degree of anisotropy of the graphite, and this trend was stronger for small batches than for large ones.

An increase in batch size usually increased bulk density, binder carbon residue, Young's modulus, and degree of anisotropy, although in general these changes were neither as large nor as consistent as those produced by changing the binder.

In large batches of graphite made using EMW 1600 resin, some structural imperfections have been observed microscopically, mainly in the forms of centrally located axial crack systems, small joined microcracks, and strings of pores. These appear not to have been seriously damaging to the properties of the graphites, since the highest strengths and densities so far observed were measured on these graphites. At least in part they may have resulted from a pronounced increase in viscosity of the EMW resin which occurred at some unknown time during the last several months. (A new procedure for storing and using such resins has been established to avoid the possibility that undetected changes of this type will influence future results.) However, experiments have been undertaken to determine why and at what stage of manufacture or heat treatment these defects were produced.

Graphite ACE4, made as a large batch from G-18 (Great Lakes 1008-S) graphite flour, Thermax carbon black, and EMW 1600 graphite flour, was found microscopically to contain some microcracks parallel to the extrusion axis. However, its physical properties were quite uniform, and it was selected for tensile testing and density evaluation. The unmachined rod (approximately 0.475 in. dia) tested in 4-in. lengths gave an ultimate tensile strength of 3235 psi with standard deviation of 271 psi. Specimens machined to 0.250-in. dia in the center of the gage section with large end radii gave an ultimate tensile strength of 4775 psi with standard deviation of 207 psi. This is the highest strength so far reported for a CMF-13 extruded graphite.

Densities were measured on the ACE4 rods from which the tensile bars were machined. Measurements were made on full-length bars, on 1/3-length bars, on 1/2-length bars from which a skin 0.020-in. thick had been removed, and on 1/3-length bars machined to 0.250-in. dia, with the results listed in Table XI. There is a trend toward higher density away from the surface of the extrusion, which indicates that the exteriors of the rods were slightly more porous than their interiors. This would be expected to cause some change in strength with specimen diameter, but not the large change noted above. Evidently either the specimen used or the testing procedure for full-diameter specimens gives misleadingly low values.

B. Effects of Catalyst Concentration (J. M. Dickinson)

The effect of the concentration of curing catalyst added to Varcum 8251 binder resin was discussed briefly in Report No. 3 in this series. Up to a point, an increase

TABLE XII

COMPOSITIONS AND EXTRUSION CONDITIONS OF ZrC-GRAPHITE COMPOSITES

Sample Number	ZrC Content		Binder Increment[c]	Extrusion Conditions					Green Diameter, in.	Comments on Mix Texture
	Weight Ratio[a]	Weight Fraction[b]		Pressure, psi	Velocity, in./min	Temperature, °C		Vacuum, Torr		
						Mix	Chamber			
ACP4	0.10	0.091	0.257	3825	164	45	50	450	0.5035	Wet
ACP5[d]	0.10	0.091	0.257	6120	171	56	45	400	0.5005	Wet
ACP6	0.20	0.167	0.257	4050	180	41	45	450	0.5025	Wet
ACP7	0.30	0.231	0.257		160	53	48	500	0.5055	Wet
ACP8	0.40	0.286	0.056	5625	157	43	49	650	0.504	Dry
ACP9	0.50	0.333	0.060	5670	164	43	43	700	0.506	Dry
ACP10	0.60	0.375	0.104	4050	164	45	49	<900	0.504	OK
ACP11	0.67	0.402	0.111	3825	171	44	51	<900	0.503	Wet (?)
ACP12	0.77	0.435	0.113	3375	171	43	53	900	0.502	A little wet
ACP13	0.87	0.466	0.105	3825	171	47	48	600	0.504	A little wet
ACP14	0.97	0.493	0.097	3600	157	48	49	>1000	0.5035	OK
ACP15	0.05	0.048	0.057	4950	164	48	48	>1000	0.5055	Dry
ACP16	0.025	0.024	0.057	5625	164	45	50	700	0.5025	OK
ACP17	0.125	0.012	0.114	4725	171	46	48	1000	0.506	OK
ACP18	0.006	0.006	0.000	4500	171	47	46	1000	0.506	OK

(a) Ratio by weight of ZrC to graphite filler (85 parts G-18 plus 15 parts Thermax).

(b) Fraction of total filler (ZrC plus G-18 plus Thermax) that is ZrC.

(c) Grams of binder added per gram of ZrC in addition to 27 pph required for the graphite.

(d) ACP5 was made using EMW 1600 binder; all others were made with Varcum 8251.

in catalyst concentration increases the carbon residue realized from the binder and the bulk density of the finished graphite. However, if too much catalyst is used the polymerization reaction occurs too rapidly, which can damage the graphite during curing or even cause the mix to "set" before or during extrusion.

Graphites made from high-viscosity furfuryl alcohol resins have shown some tendency toward cracking, particularly when made in large batches. It was thought possible that the cracking occurred during curing and resulted from use of too high a concentration of catalyst. Accordingly, three lots of extruded graphite were made from 85 parts G-18 (Great Lakes 1008-S) graphite flour, 15 parts Thermax carbon black, and EMW 1600 furfuryl alcohol resin catalyzed in one case with the usual 4% of maleic anhydride and in the others with 3% and with 2% of maleic anhydride. The graphites with 4% and 2% of catalyst were heat-treated together. That containing 3% of catalyst was made more recently, after a distinct increase in resin viscosity had occurred, and may not be directly comparable with the other two.

Graphite ACE5, in which the binder contained 4% catalyst, had bulk density of 1.905 g/cm^3, binder carbon residue of 49.2%, and electrical resistivity of 1086 μΩcm. Graphite ACE6, in which the binder contained only 2% catalyst, had bulk density of 1.887 g/cm^3, binder carbon residue of 47.4%, and electrical resistivity of 1119 μΩcm. No differences were detected microscopically between the two graphites.

It appears that in this case no benefit was obtained from lowering the concentration of maleic anhydride catalyst from 4% to 2%, and that some degradation of graph-

TABLE XIII

CRYSTALLINE PARAMETERS AND PROPERTIES OF HEAT-TREATED POCO GRAPHITES

Specimen No.	Original Poco Grade	Bulk Density, g/cm³	Void Fraction	Crystalline Parameters d_{002}, Å	Crystalline Parameters L_c, Å	Crystalline Parameters Anisotropy, M[a]	Thermal Conductivity, W/cm-K	Electrical Resistivity, μΩ cm
15	AXZ-9Q	1.539	0.316	3.365	430	0.10	0.70	1949
14	AXZ	1.544	0.314	3.364	435	0.01	0.75	1921
5	AXZ-QBG	1.625	0.278	3.364	420	0.17	0.89	1615
8	AXZ-QB	1.631	0.275	3.366	375	<0.01	0.92	1585
11	EP-1924	1.753	0.221	3.367	360	0.16	1.07	1220
12	AXM-9Q	1.756	0.220	3.368	350	0.12	1.11	1337
10	EP-1924	1.766	0.215	3.367	355	0.07	1.25	1133
13	AXM-9Q	1.767	0.214	3.367	355	0.09	1.14	1350
9	EP-1924	1.773	0.212	3.367	350	0.04	1.18	1144
2	AXF-5Q	1.788	0.205	3.367	350	0.12	1.16	1183
1	AXF-5Q	1.817	0.192	3.368	350	0.04	1.29	1237
3	AXF-QBG	1.834	0.185	3.368	330	0.01	1.35	1068
6	AXF-QB	1.896	0.157	3.368	335	0.09	---	986
4	AXF-QBG	1.900	0.156	3.368	325	0.07	---	1018
7	AXF-QB	1.904	0.154	3.368	325	0.01	1.73	987

a) Maximum anisotropy, from $I(\phi) = I_o \sin^M \phi$.

ite properties resulted from the change.

The graphite made with 3% maleic anhydride catalyst had bulk density of 1.914 g/cm³, binder carbon residue of 48.8%, electrical resistivity of 1096 μΩcm, and Young's modulus of 2.66×10^6 psi. Because of the change in binder viscosity with time, it is not clear that the high density of this material was due to the catalyst concentration used. The possible desirability of reducing the maleic anhydride concentration from 4% to 3% in high-viscosity furfuryl alcohol resins will therefore be determined in a future experiment of this type.

VI. GRAPHITE-CARBIDE COMPOSITES

A. Extruded Graphite-ZrC Composites (J. M. Dickinson)

For use in a study of the relationship between thermal conductivity and thermal diffusivity, a heterogeneous material is required. A particulate composite containing various proportions of ZrC particles in a graphite matrix has been selected for this purpose. It is desirable that the graphite matrix remain essentially the same while the ZrC content is increased from zero to above 50% by weight.

The ACP series of composite extrusions has been made to study binder requirements, fabrication and heat-treating problems, and the quality and uniformity of the rods produced. The mix consisted of 85 parts C-18 (Great Lakes Grade 1008-S) graphite flour, 15 parts Thermax carbon black, a variable proportion of ZrC powder, and Varcum 8251 furfuryl alcohol resin binder containing 4% maleic anhydride curing catalyst. The binder concentration was 27 ppb relative to the graphite filler (graphite flour plus carbon black) with additional binder added to coat the ZrC particles. Compositions and extrusion conditions are given in Table XII.

From the data of Table XII, it appears that the binder requirements of these composites will be about 0.1 g

resin per gram of ZrC in addition to the 27 ppb required for the graphite matrix. It also appears that binder concentration may be critical, since additions only slightly greater or less than this made the mix appear to be either too wet or too dry. Some further adjustments of binder requirements may be indicated by property data when they become available.

Extrusion pressures remained rather low for this series of composites, and green diameters were typical of the graphite without additions. Extrusion ACP5 was made using EMW 1600 binder instead of Varcum 8251, and of course had the highest extrusion pressure and the smallest green diameter.

Properties are now being determined on this series of composites.

VII. EFFECTS OF POROSITY ON GRAPHITE PROPERTIES

A. Previous Work

The effects of porosity on the elastic properties of Poco and Santa Maria graphites have previously been discussed in Reports No. 11, 12, and 13 in this series. Preliminary results on the effect of porosity on the thermal conductivities of heat-treated Poco graphites were described in Report No. 13.

B. Heat-Treated Poco Graphite Samples

In order to isolate unambiguously the effects of porosity, it is necessary to have available a series of specimens in which fractional porosity is the only significant variable and the graphite matrices are essentially identical. In an attempt to produce such a series, fifteen specimens of Poco graphite of varying density were heat-treated together in flowing helium at 2900°C, which is believed in all cases to exceed the graphitizing temperature originally used by the manufacturer. It was expected that this would eliminate differences in the matrix structures due to variations in their previous thermal histories.

The bulk densities of the fifteen heat-treated specimens ranged from 1.539 to 1.904 g/cm³, corresponding to void fractions of 0.316 to 0.154.

X-ray parameters of these specimens, determined by J. A. O'Rourke, CMF-13, are listed in Table XIII. The degree of crystalline perfection, as indicated both by interplanar spacing, d_{002}, and by mean crystallite thickness, L_c, was slightly higher for the lower-density materials, although the differences were not large. Because adjacent orthogonal sections were not available, crystalline anisotropies could be measured only as M-values. Each sample was examined in several azimuthal directions, and in each case the M-value representing the direction of greatest anisotropy was determined. While these maximum values are listed in Table XIII, the average value for each sample was 0.04 or less.

Although minor variations in x-ray structure were detected, these differences were small, and all specimens were very nearly isotropic. Certainly the major variable in this series of graphites is density.

C. Elastic Properties (P. E. Armstrong)

By extrapolating the curve of elastic modulus vs void fraction to zero void fraction, an apparent modulus for theoretically dense material can be determined. The slope of the curve is a measure of the effectiveness of the voids in reducing elastic modulus. For the Poco graphite samples described above, the slopes of the modulus vs void fraction curves were greater than were those of similar curves for powder-metallurgy tungsten, indicating that in the graphite the voids were more effective in reducing the elastic properties. The same conclusion was reached by fitting the two sets of data to a modified Mackenzie equation.

The ratio of Young's modulus to shear modulus was nearly the same for all of the graphite samples, indicating that the type and character of the porosity did not change as the amount of porosity increased. As is indicated in Table XIV, elastic moduli at theoretical density (determined by extrapolation, as described above) are much lower for Poco graphite than for single-crystal tungsten, but the relations between the various moduli are very nearly the same for the two materials.

Since the Mackenzie theory apparently allows for a

TABLE XIV

PREDICTED ELASTIC MODULI OF THEORETICALLY DENSE, 2900°C-ANNEALED, POCO GRAPHITE COMPARED TO THOSE OF SINGLE-CRYSTAL TUNGSTEN

	Poco Graphite	Tungsten Single Crystal
Young's Modulus, E, psi	2.95×10^6	59.3×10^6
Shear Modulus, G, psi	1.14×10^6	23.0×10^6
Bulk Modulus, K, psi	2.33×10^6	46.9×10^6
Ratio, G to E	0.388	0.388
Ratio, K to E	0.790	0.791

distribution of pore sizes, the conclusion can be drawn that the effect of void fraction on elastic properties of graphite and of tungsten is different because of differences either in pore shape or in particle anisotropy.

Extruded graphites made from Santa Maria fillers seem to have the same density-modulus relation found for the heat-treated Poco graphites, and to correlate well with molded Santa Maria graphites in this regard.

D. Thermal Conductivity (P. Wagner)

B. N. Ivanov (Teplofizika Vysokikh Temperatur 4, 875, 1966) has suggested that in any porous, dielectric, crystalline material, the effects of pores on thermal conductivity will be manifested as a scattering of phonons and electrons. Graphite is not a dielectric, and at this time it is felt that the thermal conductivity of graphite is describable in terms of a phonon-scattering mechanism only. However, it appears that Ivanov's ideas may be applicable to phonon-scattering by voids in polycrystalline graphite.

The traditional kinetic-theory expression for thermal conductivity, λ, is

$$\lambda = \frac{1}{3} \sum_{i=1}^{n} C_i V_i \ell$$

where C = heat capacity
V = phonon velocity
ℓ = mean free path
i = accoustic mode index.

Application of Mathiessen's rule to thermal resistances yields

$$\frac{1}{\ell} = \sum_{j=1}^{n} \frac{1}{\ell_j} = \frac{1}{\ell_{BS}} + \frac{1}{\ell_U} + \frac{1}{\ell_{pores}} + \cdots$$

where the subscripts BS and U indicate boundary scattering and Umklapp scattering respectively. From Ivanov's work

$$\ell_{pores} \sim 1/NX^2$$

where N is the number of pores per unit volume and X^2 is the scattering cross-section per pore.

In the case of the samples discussed above, an attempt was made to keep the graphite structure constant except for the pores. If this was accomplished, any changes in the observed thermal conductivity should be due only to changes in ℓ_{pores}, and

$$\lambda \sim \ell_{pores} \sim 1/NX^2.$$

Considering heat conduction across a plane, where N' is the number of pores per unit area and X^2 is the mean scattering cross-section of the pores in that plane, $N'X^2$ is just the two-dimensional void-fraction, which can be expressed in terms of density as follows:

$$\lambda \sim 1/(\text{void fraction}) = \delta_{th}/(\delta_{th} - \delta)$$

where δ_{th} is the theoretical density of graphite and δ is the observed density of the graphite sample. Thus, for the samples of heat-treated Poco graphite, if C_i and V_i are constant, a plot of λ vs reciprocal void fraction should yield a straight line.

Thermal conductivities of the Poco graphite samples described above have been measured at room temperature by the flash-diffusivity method, and are plotted in Fig. 10 as a function of reciprocal void fraction. Indeed the data are well represented by a line, and again it appears that the only significant difference among the samples was in their fractional porosities.

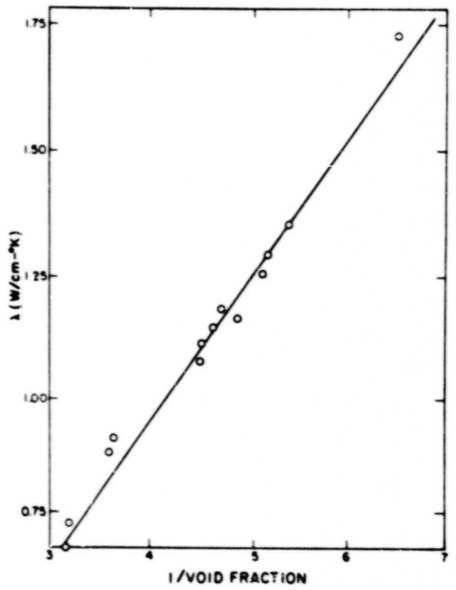

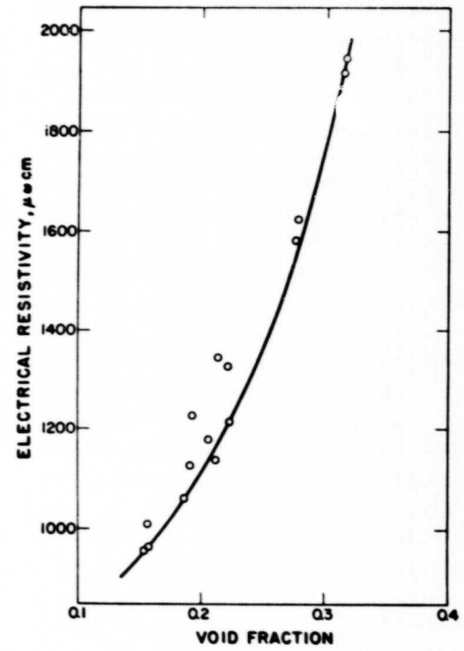

Fig. 11. Effect of porosity on the electrical resistivity of 2900°C-annealed Poco graphites.

E. Electrical Resistivity (P. Wagner)

The electrical resistivities of the heat-treated Poco graphite specimens have also been measured, and the data examined in the light of Ivanov's paper. His formulation suggests that electrical resistivity should vary with porosity in the same way as does thermal resistivity--that is, that electron-scattering and phonon-scattering are similarly affected. If this were the case, electrical conductivity, σ, would also be a linear function of reciprocal void fraction, which it is not. If, however, a simple density correction is made such that

$$\sigma_{th} = \sigma_{obs}(\delta_{th}/\delta) = \sigma_{obs}/(1-P)$$

where σ_{th} = corrected electrical conductivity
σ_{obs} = measured electrical conductivity = $1/\rho_o$
P = void fraction

Then ρ_R, the electrical resistivity corrected to theoretical density, will be given by

$$\rho_R = \rho_o - \rho_o P$$

Where ρ_o is the measured electrical resistivity. A plot of ρ_o vs P from this relation should give a curve which is concave upward.

Electrical resistivities of the Poco graphite samples are plotted in this way in Fig. 11. There is considerable scatter in the data. However, if the viewpoint is taken that any structural flaw in the material or indeterminate error in the measurement must yield a resistivity value which is higher than the value truly representative of the material, then the best curve is the one that goes through the smallest measured values of ρ_o. Such a curve has been drawn in Fig. 11, and is indeed concave upward.

Concern has been expressed in the literature with regard to the effects of pore shape and orientation on scattering. In the limit, the expression for electrical con-

ctivity might have the form

$$\sigma_{th} = \frac{\sigma_0}{1 - aP}$$

here a is an adjustable parameter (Loeb, A. L., J. m. Cer. Soc. 37, 96, 1954) whose value would reflect e scattering effectiveness of the pore structure.

The different effects of porosity on the thermal and ectrical conductivities of the annealed Poco graphites ppear to indicate that phonon-scattering is the important echanism in thermal conduction and that electron-scat-ring--by a different mechanism--is the important one electrical conduction. In this regard it is of interest examine the behavior of a system in which the natures the carriers are better understood. The effects of po-osity on the thermal and electrical conductivities of ngsten, in which heat conduction is known to be about % electronic in nature, have been described in the lit-rature (Kalcinski, G. L., Wagner, P., and Cowder, . R., J. Less Common Metals 7, 383, 1964). Since th λ and σ are controlled by electronic processes, eir dependence on void fraction should be the same and hould also be the same as that observed for σ in graph-e. In the case of tungsten this is indeed the experimen-l observation.

VIII. SKIN EFFECTS IN GRAPHITE

(P. Wagner)

"Skin effects" are often reported for graphites, for ample in connection with the tensile tests discussed arlier in this report. To explore the magnitude of such effect, an experiment has been performed in which lectrical resistance (parallel to the extrusion axis) was easured on an as-fabricated rod of CMB-13 lot AAQ1 raphite, the rod was machined to successively smaller iameters, and electrical resistance was measured after ach machining step. Considering the observed resist-nce to be the resultant of the parallel resistances of a uccession of nested, concentric, graphite tubes, the re-istance of each tube was calculated from

$$\frac{1}{R} = \sum_{i=1}^{n} \frac{1}{R_i}$$

where n is the number of tubes considered plus one (the cylindrical core). From these results the "true" resistivity of each imaginary tube was calculated, and has been plotted in Fig. 12 as a function of radial distance from the center of the rod. (The original rod radius was 0.2375 in., and radial position is given as a fraction of this distance, measured from the axis of the rod.)

From Fig. 12 it is seen that the electrical resistivity of the graphite is highest at the surface of the sample and decreases continuously toward its center. This is probably not a result of the existence of a higher degree of preferred orientation of filler particles near the surface--although that situation is believed to exist. Extrusion produces a preferred orientation in which the layer planes of the graphite structure, which contain the directions of minimum electrical resistivity, are inclined to the surface at a low angle. A high degree of preferred orientation therefore results in relatively low with-grain resistivity, which is not the situation near the surface of the AAQ1 graphite rod. Accordingly, relatively high resistivity near the surface of the rod must in this case apparently be explained in terms of a higher concentration of defects there. These defects may be voids, from loss of volatile matter through the surface layers, or cracks produced by contraction stresses, which would tend to be highest near the surface, or some combination of the two. Empirically, when the resistivity data are plotted against the square of the radial distance, they are reasonably well represented by a line (Fig. 13). This would be consistent with a diffusion mechanism of some kind involved in formation of the defects.

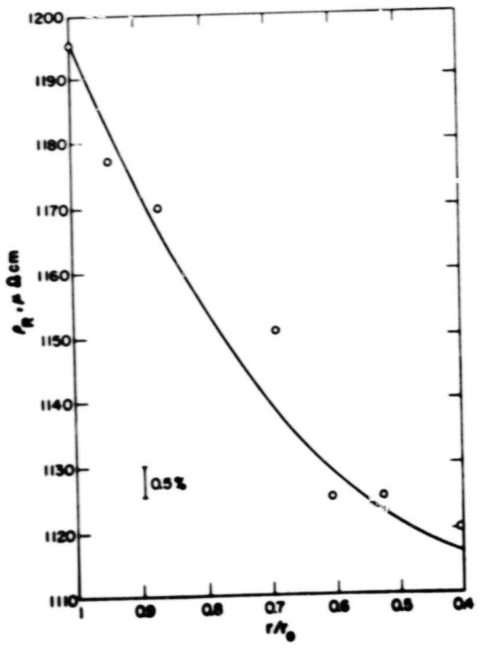

Fig. 12. With-grain electrical resistivity of AAQ1 graphite, rod No. 134, as a function of radial position.

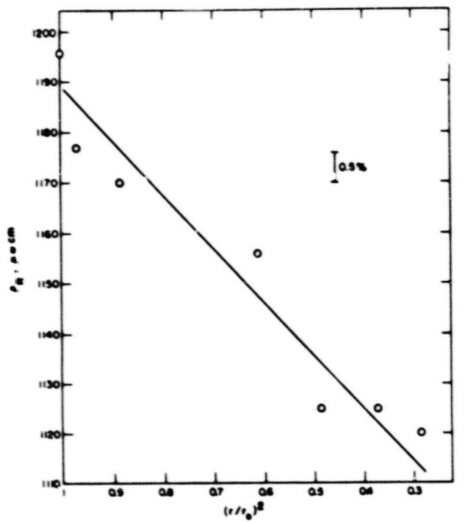

Fig. 13. With-grain electrical resistivity of AAQ1 graphite, rod No. 134, as a function of the square of radial distance from the rod axis.

There is also a skin-effect on the thermal expansion of AAQ1 graphite measured in the with-grain direction. The as-fabricated rod, with the extrusion skin intact, had an average thermal-expansion coefficient (25-645°C) of 2.46×10^{-6}/°C. After removal of about 0.005 in. of surface material from the rod radius, the average coefficient was 2.89×10^{-6}/°C. Further graphite removal appeared to have no effect. Apparently, since there was no gradient of thermal expansion at greater depth, the skin effect on thermal expansion has a different cause than does that on electrical resistivity. The effect on thermal expansion is consistent with the presence of a highly oriented surface layer on the graphite, whose effect on electrical resistivity was apparently overwhelmed by other aspects of the graphite structure.

IX. GRAPHITIZATION

A. Graphitization of Furfuryl Alcohol Resin (R. D. Reiswig, E. M. Wewerka)

A sample of an experimental, high-viscosity, furfuryl alcohol resin, CMF-13 lot EMW 1600, was cured at 60°C for 30 days, after which it was still slightly deformable. Small particles and spheres of vitreous carbon were forced into its surface while it was still warm, and the sample was then baked and graphitized in normal cycles. Microscopic examination of the sample after the graphitizing heat-treatment showed that, where the resin had been deformed by indentation by the particles, optical anisotropy had developed and lamellar structures--indicating graphitization--had appeared, with the basal planes of the graphite aligned parallel to the surfaces of the indentations. Elsewhere the structure of the heat-treated carbon residue was optically isotropic and featureless, as would be expected of a vitreous carbon.

This observation supports the concept that the graphitization of a furfuryl alcohol binder residue, which occurs when it is associated with a filler, results from the mechanical strain that occurs when the resin shrinks around an essentially incompressible filler.

B. Graphitization of Needle Coke (R. J. Imprescia, J. A. O'Rourke)

Crystalline parameters have been determined for samples of a needle coke which were heat-treated individually at temperatures up to about 2700°C. The coke investigated was Union Carbide Corporation No. 1 Needle

TABLE XV

CRYSTALLINE PARAMETERS OF HEAT-TREATED NEEDLE COKE, CMF-13 LOT CNI-1

Heat-Treatment Temperature	L_c, Å	d_{002}, Å
As-Received	52.8	3.45
1230°C	68.5	3.435
1520°C	104	3.430
1825°C	217	3.418
2130°C	280	3.395
2420°C	427	3.374
2715°C	670	3.362

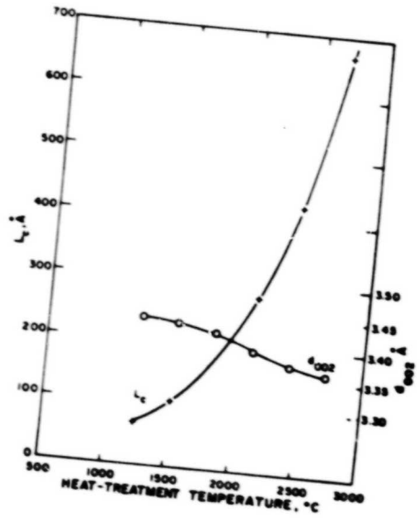

Fig. 14. Crystalline parameters of a needle coke, CMF-13 Lot Nc. CNI-1, as functions of heat-treating temperature.

Coke, CMF-13 Lot No. CNL-1. The heat-treatments were performed in the static "carbonaceous" atmosphere produced by packing crucibles containing the coke samples in carbon black. Results of the x-ray measurements are listed in Table XV and plotted as functions of heat-treating temperature in Fig. 14. The curve of interplanar spacing, d_{002}, vs heat-treating temperature is very similar to that of Santa Maria coke. The curve of mean crystallite thickness, L_c, vs heat-treating temperature is displaced upward (to higher L_c values) from that for Santa Maria coke, has greater slope at temperatures above about 2400°C, and is still rising rapidly at 2700°C, where the curve for Santa Maria coke has begun to flatten.

X. PUBLICATIONS RELATING TO CARBONS AND GRAPHITES

Smith, M. C., "CMF-13 Research on Carbon and Graphite, Report No. 13, Summary of Progress from February 1 to April 30, 1970", LASL Report No. LA-4480-MS, July, 1970.